



Asian Research Association

INTERNATIONAL RESEARCH JOURNAL OF MULTIDISCIPLINARY TECHNOVATION



BN+SiC Hybrid Nanofluid in Enhanced Microchannels: Numerical Heat Transfer Augmentation Study

Anirban Bose ^{a, *}, Arunabha Chanda ^a

^a Department of Mechanical Engineering, Jadavpur University, Kolkata, India

* Corresponding Author Email: aboserresearch@gmail.com

DOI: <https://doi.org/10.54392/irjmt2612>

Received: 19-05-2025; Revised: 13-11-2025; Accepted: 20-11-2025; Published: 10-12-2025



Abstract: This research article numerically investigated the performance of non-oxide hybrid Boron Nitride Silicon Carbide (BN+SiC/water) hybrid nanofluid in high heat flux miniaturized electronic hardware. 3d-CFD model validated with established experimental data on a triangular section, oblique microchannel geometry is used to explore the influence of total particle loading (0.5 to 1.5 %), relative particle proportion, on the Nusselt number (Nu), friction factor (f) and thermal performance factor (TPF). The results compared with the benchmark conventional oxide hybrid nanofluid system (Al₂O₃+CuO/water) and found superior on overall thermo-hydraulic performance. Heat transfer enhancement by 50% with respect to base fluid water, is quite an improvement in thermal enhancement, if we compare with the benchmark oxide system reference of around 37%. It is also observed that relative SiC proportion increases the performance of this system. Nanoparticle size and morphology effects on the thermo-hydraulic performance is also studied in this work. Smaller size particles are found beneficial in a quantitative analysis in the range of 10nm to 90nm average particle diameter. Non spherical high aspect ratio shapes nanoparticles enhance the performance of the nanofluid observed in this study. This study not only introduced a novel advanced heat transfer fluid but also allow the design customization insight for this BN+SiC/water hybrid nanofluid system.

Keywords: Hybrid Nanofluid, BN+SiC, Microchannel, Heat Transfer Enhancement, Particle Shape Effect, Particle Size Effect, Numerical Simulation, Thermo-hydraulic Performance, Nanoparticle Morphology

1. Introduction

Recent shift of the technology towards the cloud servers, data centers and other automation-based equipment hardware have made the thermal management a primary design challenge to the scientists and engineers [1, 2]. Efficient heat dissipation from the power electronics and battery hardware present inside electric vehicles is an acute problem in automotive sector. Requirement of faster charging system increases the power densities which make the efficient cooling system design very challenging [3]. Inefficient design of thermal management system can lead to a catastrophic failure of the hardware [4]. Constant increasing demand of cooling in massive heat flux of highly integrated electronics is not possible with conventional coolants because of their low thermal conductivity [5]. Microchannel heat sinks having very high area to volume ratio, suitable for high heat dissipation rate, is a passive solution strategy [6, 7]. Design optimization of microchannel geometry is crucial but not potential enough to meet the cooling requirement required. A parallel advancement in the working fluids themselves are also essential [8].

Nanofluid as a coolant advances the heat transfer technology promisingly for last two decades [9].

Nanofluids are the dispersed high thermal conductivity nanoparticles (like Al₂O₃, CuO) within a conventional base fluid having superior heat transfer capabilities [10, 11]. Many studies reported that a small concentration of nanoparticles can enhance the heat transfer capacity of nanofluid a significant amount and make it suitable as a heat transfer fluid [12, 13]. But lacking of stability of nanofluid causes blockage in the flow path and diminished thermal efficiency limits their widespread commercial adoption [14, 15]. Addition of nanofluid increases pumping power required to maintain the flow rate which can't be ignored when implemented in practice [16].

Researchers explored hybrid nanofluids, which combines two or more different types of nanoparticles. A carefully chosen combination produced synergistic effects, enhancing thermal properties even further while mitigating some of the drawbacks of single-component systems. Most of the work has centered on metal oxide hybrids, with systems like Al₂O₃-CuO/water demonstrating thermal performance superior to their single-component counterparts [17, 18]. MWCNT-SiO₂ hybrids showed a noticeable enhancement in heat transfer with a negligible pressure drop penalty [19]. These oxide-based systems, including the work by

Vinoth and Sachuthanathan [20], provide benchmarks for validating CFD models.

Non-oxide ceramics like silicon carbide (SiC) and boron nitride (BN) are highly potential candidates for heat transfer application because of their unique thermophysical properties. Recent studies reveal that BNs having high intrinsic thermal conductivity and ability to enhance convective heat transfer coefficient when used in a nanofluid. But the long-term stability issues were there and addressed by the researchers through surface modification techniques [21-23]. Similarly, experiments with SiC nanofluids have demonstrated notable performance gains in applications ranging from plate heat exchangers to microchannel machining [24, 25]. Few recent studies reported the promising hybrid non-oxide Cu-Graphene [26] and h-BN/SiC nanofluid tailored for specialized grinding processes [27]. A systematic investigation into an aqueous BN+SiC hybrid nanofluid designed specifically for microchannel heat transfer remains largely unaddressed. This is an opportunity for further research in this area to fill this research gap.

This gap becomes even more critical when one considers the parallel evolution of microchannel design. Passive enhancement of thermal efficiency can be achieved in microchannel geometry by integrating features like grooves, ribs or wavy flow paths. In this way intentionally thermal boundary layers are disrupted and introduced secondary flows which promote mixing and augment convective heat transfer coefficient [28-30]. Microchannels that incorporate oblique or triangular elements fall into this category of enhanced geometries. These geometric modification improves thermal performance but at the cost of high pressure drop [31-32]. An optimal solution of right type of nanofluid selection along with modified geometry is a key challenge to balance the increased hydraulic resistance and enhanced heat transfer benefit [33, 34]. Combination of novel non-oxide hybrid nanofluid BN+SiC with complex geometry of flow passages in heat sink design is largely unexplored. Understanding of this potential, high-performance advanced cooling system for the next generation thermal management systems is not clear at this time. There is a clear need for a systematic analysis of how nanoparticle properties, especially morphology and concentration, influence the delicate equilibrium between enhanced heat transfer and increased friction losses within these advanced channel designs.

The primary aim of this research is detailed numerical study and optimization of the combined interaction of microchannel enhanced geometry and non-oxide hybrid advanced nanofluid. A single phase, laminar and conjugate heat transfer CFD model of complex geometry is prepared and validated against published experimental data for oxide based nanofluid. This model is then used to investigate the performance

of BN+SiC/Water hybrid nanofluid over a range of operating conditions and parameters of the cooling system to find the relation and synergic effect in terms of thermo-hydraulic performance parameters. A comprehensive parametric analysis will form the core of this study, examining how key nanoparticle characteristics including particle size, total volume concentration, the blending ratio of BN to SiC, and even particle shape impacts the system's overall thermo-hydraulic performance. By evaluating these effects in terms of friction factor, average Nusselt number, and the resulting thermal performance factor, we hope to provide a much clearer picture of how particle-level properties translate into macroscopic system behavior. Finally, the results for BN+SiC hybrid nanofluid are compared with benchmark results of Al_2O_3+CuO system. This work provides a clear actionable insight to customize the advanced cooling system described for specific application.

2. Materials and Methods

This section elaborates the model geometry, mesh, governing mathematical framework of the numerical scheme and model validation with established experimental results, implies the numerical methodology used to study the thermo-hydraulic performance of BN+SiC/Water hybrid nanofluid flowing through a triangular section oblique microchannel. Detail material properties and relations are included in this section. A detailed parametric study plan is also provided in this chapter.

2.1 Numerical Analysis

2.1.1 Geometry

A 1:5 scaled down geometry model of the physical model of the experimental work by Vinoth and Sachuthanathan [20] is used to ensure computational feasibility without sacrificing crucial flow characteristics for the CFD analysis in our study. Complex channel geometry specifications are provided in the Table 1. The flow path is oblique microchannel with triangular section as shown in Figure 1(a).

Table 1. Triangular microchannel geometry specification [20]

Parameters	Triangular Microchannel Measurement
Fin width (mm)	0.900
Fin depth (mm)	0.900
Fin length (mm)	0.950
Fin pitch (mm)	0.800
Oblique angle (deg)	26

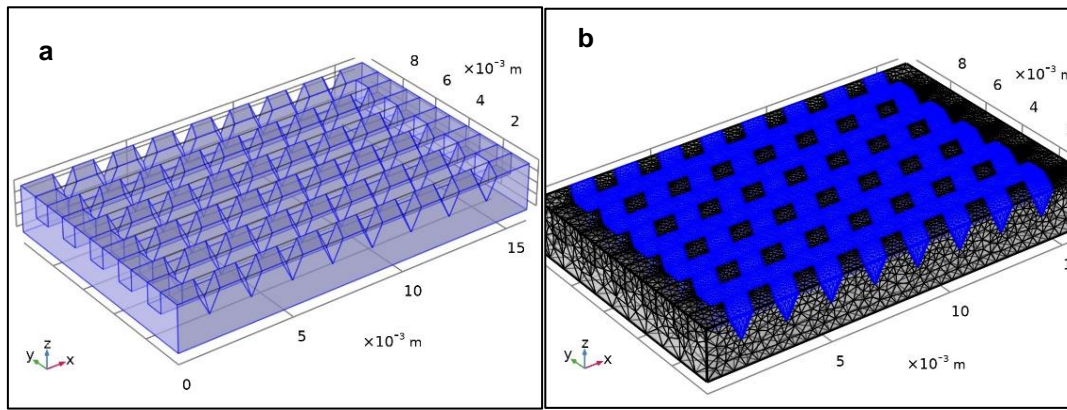


Figure 1 (a) 3D Geometry of the microchannel with triangular oblique sections, **(b)** Mesh details showing fluid and solid domains

3D-model analyzed in this research is captured not only the complex microchannel flow path but also the adjacent copper substrate of the plate, same as used in the actual foundation experiment. Geometry and mesh are shown in Figure 1(a) and 1(b) respectively.

2.1.2 Governing Equations

In this 3-d steady state numerical simulation of conjugate heat transfer, incompressible and laminar flow model equations (equations 1-4) [35] are solved neglecting viscous dissipation and body forces.

Continuity Equation:

$$\nabla \cdot u = 0 \tag{1}$$

Momentum Equation (Navier-Stokes):

$$\rho_{nf}(u \cdot \nabla)u = -\nabla p + \mu_{nf}\nabla^2 u \tag{2}$$

Energy Equation (Fluid Domain):

$$\rho_{nf}c_{nf}(u \cdot \nabla)T_f = k_{nf}\nabla^2 T_f \tag{3}$$

Energy Equation (Solid Domain):

$$k_s\nabla^2 T_s = 0 \tag{4}$$

Where u =velocity vector, p =pressure, T =temperature, ρ =density, μ =dynamic viscosity, c_p =specific heat capacity at constant pressure, and k =thermal conductivity. The subscripts 'nf', 'f', and 's' denote nanofluid, fluid, and solid, respectively.

2.1.3 Numerical modeling approach: single phase analysis

In this study nanofluids are assumed to be uniform, homogeneous and continuous medium with equivalent single phase thermophysical properties obtained from established correlations (equations 5-9) with the properties of each phase and their concentration. These single-phase assumption of the nanofluid is not only computationally favorable for its simplification but also produces quite accurate predictions for dilute nanofluid systems with little particle

migration and interphase slip has been validated [36]. The successful application of this methodology hinges on the precise calculation of the nanofluid mixture's effective characteristics.

Maximum nanoparticle concentration in our study was 1.5% suitable for improved thermophysical properties of nanofluid as heat transfer fluid. But definitely there is a chance of two-phase interaction effects may incur error in the single-phase assumption. This can be taken up as a future scope to study the two-phase analysis for higher concentration and comparing with single-phase results to obtain a comparative phase transition insight.

2.1.4 Effective properties

Single-phase equivalent properties of the oxide based nanofluids (Al_2O_3 /water and Al_2O_3+CuO /water) for validation and non-oxide based hybrid nanofluid (BN+SiC/water) for the current study are calculated using the established models and correlations based on the base fluid (water) and constituent nanoparticles' (BN, SiC, Al_2O_3 , CuO) properties. Isotropic average thermal conductivity of anisotropic hexagonal boron nitride (h-BN) has been used to reduce the computational expense and this aligns with established single-phase modeling of dispersed randomly oriented nanoparticles without much error. Anisotropic thermal behavior can be investigated and compared with this result in future work to get a deep understanding of shape and particle orientation effect. The volume fraction of nanoparticles (ϕ) is a key parameter. For hybrid nanofluids, the properties depend on the total volume fraction ($\phi_{total} = \phi_{np1} + \phi_{np2}$) and the individual fractions of each nanoparticle type. The effective density (ρ_{nf}) and specific heat capacity ($c_{p,nf}$) are calculated using the mixture rule [37, 38] shown in equation (5) and (6).

$$\rho_{nf} = (1 - \phi_{total})\rho_{bf} + \phi_{np1}\rho_{np1} + \phi_{np2}\rho_{np2} \tag{5}$$

$$(\rho c_p)_{nf} = (1 - \phi_{total})(\rho c_p)_{bf} + \phi_{np1}(\rho c_p)_{np1} + \phi_{np2}(\rho c_p)_{np2} \tag{6}$$

The effective dynamic viscosity (μ_{nf}) is estimated using classical models like the Brinkman model [39], which is commonly used for dilute suspensions for spherical particles shown in correlation (7a).

$$\mu_{nf} = \frac{\mu_{bf}}{(1-\varphi_{total})^{2.5}} \tag{7a}$$

$$\mu_{nf} = \mu_{bf} \left(1 - \frac{\varphi_{np1}}{\varphi_{max}}\right)^{-n_{np1}} \left(1 - \frac{\varphi_{np2}}{\varphi_{max}}\right)^{-n_{np2}} \tag{7b}$$

Considering the effect of the nanoparticle shape effective viscosity is calculated based on the Krieger-Dougherty modified equation model [40] for hybrid nanofluid shown in correlation (7b). Where, n_{np1} and n_{np2} are shape factors defined as $n = \frac{3}{\psi}$, for each nanoparticle shape and ψ is sphericity of the nanoparticle shape defined as ratio of surface area of sphere of same volume with actual surface area of the particles. For spherical nanoparticles $\psi = 1$ and $n = 3$. φ_{max} in the correlation indicates the maximum packing fraction of the nanoparticles. Typical values of the n and φ_{max} for BN [41] and SiC nanoparticles [42] are shown in Table 2.

The effective thermal conductivity (k_{nf}) is estimated using models that account for particle shape and potentially size effects. For the baseline case assuming spherical particles, the Maxwell model [43] adapted for hybrid mixtures or similar formulations can be used. For studies involving shape effects, the Hamilton-Crosser model [44] is employed as shown in equation (8). The equation (8) turns into Maxwell model for spherical nanoparticles with $n=3$.

$$\frac{k_{nf}}{k_{bf}} = \frac{k_{p,eff} + (n_{eff}-1)k_{bf} - (n_{eff}-1)\varphi_{total}(k_{bf} - k_{p,eff})}{k_{p,eff} + (n_{eff}-1)k_{bf} + \varphi_{total}(k_{bf} - k_{p,eff})} \tag{8}$$

Where $k_{p,eff} = \frac{\varphi_{np1}k_{np1} + \varphi_{np2}k_{np2}}{\varphi_{total}}$ represents an effective particle conductivity for the hybrid mixture, and effective shape factor $n_{eff} = \frac{\varphi_{np1}n_{np1} + \varphi_{np2}n_{np2}}{\varphi_{total}}$. For size-dependent studies, we have used Koo-Kleinstreuer-Li (KKL) model [45], which incorporates the effect of Brownian motion, particularly for thermal conductivity shown in the equation (9). Particles of spherical shaped only has been considered for the study of size effect.

$$k_{nf} = k_{static} + k_{Brownian} \tag{9a}$$

$$k_{Brownian} = 5 \times 10^4 \beta (\rho_{np1} c_{p,np1} \sqrt{\frac{k_B T}{\mu_{bf} d_{np1}}} + \rho_{np2} c_{p,np2} \sqrt{\frac{k_B T}{\mu_{bf} d_{np2}}}) \tag{9b}$$

Where k_{static} is calculated based on Maxwell model from equation (8) with $n=3$. In the equation (9b), β is an empirical constant, k_B is Boltzmann constant, T is temperature (K), d_{np} is diameter of nanoparticle.

The properties of the base fluid (water) are taken from standard databases [46]. The bulk properties of the nanoparticles (Al_2O_3 , CuO , BN , SiC) are obtained from CRC handbook of Chemistry and Physics [47] (see **Error! Reference source not found.**).

Table 2. Typical values of shape parameters of nanoparticles [41, 42]

Material	Shape	Aspect Ratio	Sphericity	Shape Factor	Maximum Packing Factor
Boron Nitride	Spherical	1	1	3	0.63
	Flakes	10-100	0.3-0.5	6-10	0.2-0.35
	Nanorods	5-30	0.4-0.6	5-7.5	0.25-0.4
Silicon Carbide	Spherical	1	1	3	0.63
	Nanorods	5-50	0.5-0.7	4.3-6	0.25-0.4
	Whiskers	10-100	0.3-0.5	6-10	0.2-0.3

Table 3. Bulk properties of base fluid and nanoparticles [46, 47]

Properties	bf (Water)	Al_2O_3	CuO	BN	SiC
ρ [kgm^{-3}]	995.1	3600	6500	2150	3150
μ [$kgm^{-1}s^{-1}$]	0.000855	-	-	-	-
k [$Wm^{-1}K^{-1}$]	0.62	36	18	100	180
c_p [$Jkg^{-1}K^{-1}$]	4178	769	540	800	720

2.1.5 Boundary conditions

Appropriate boundary conditions are applied to the computational domain to represent the physical constraints of the system:

- Inlet: A uniform velocity profile corresponding to the specified flow rate (ranging from 0.02 L/min to 0.1 L/min, adjusted for the 1:5 scaled geometry) and a constant inlet temperature ($T_{in} = 293.15 \text{ K}$) are imposed.
- Outlet: A pressure outlet condition with zero-gauge pressure ($P_{out} = 0$) is specified.
- Bottom Wall (Solid): A constant heat flux ($q'' = 50 \text{ kW/m}^2$) is applied to the outer surface of the bottom solid wall, simulating the heat source.
- Outer Walls (Top and Sides of Solid): These surfaces are assumed to be adiabatic ($\frac{\partial T}{\partial n} = 0$), neglecting heat loss to the surroundings.
- Fluid-Solid Interface: A no-slip condition ($u = 0$) is applied at the channel walls. Conjugate heat transfer is modeled by ensuring continuity of temperature and heat flux across the interface ($T_f = T_s$ and $k_{nf} \left(\frac{\partial T_f}{\partial n}\right) = k_s \left(\frac{\partial T_s}{\partial n}\right)$).

2.1.6 Numerical scheme

To obtain numerical solutions for the governing partial differential equations (1–4), COMSOL Multiphysics v5.5, a software package operating on the Finite Element Method (FEM) was utilized. Laminar flow and conjugate heat transfer physics is selected and incompressible steady state study was carried out. Unstructured tetrahedral mesh is selected with biasing elements numbers to capture the more datapoints near the steep velocity and thermal gradient regions along the channel walls. To get a robust pressure-velocity coupling LBB (Ladyzhenskaya-Babuška-Brezzi) stability condition is used and to implement that second order Lagrange elements for velocity components and 1st order Lagrange elements for pressure was employed. 2nd order Lagrange elements were used for temperature for accurate prediction of thermal performance. An iterative numerical solution of conservation equations was achieved by a segregated solver. The solution process was converged when the scaled residuals for all governing equations consistently found below a threshold of 10^{-6} .

2.1.7 Grid Independence Study

Grid independent study ensures that simulation results are not depending on the element size and at the same time it is required to reduce the computational expense. A series of mesh densities from coarse to fine are used to carry out a specific simulation and results are analyzed to decide the minimum number of elements can be taken for the rest of the work without much error

due to size variation. Average Nusselt number (Nu) and pressure difference (ΔP) along the channel length are calculated in the postprocessing based on the solution field data obtained in the simulation. Figure 2 is the graphical presentation of the grid independent study for $\text{Al}_2\text{O}_3/\text{water}$ nanofluid at a 1% volume fraction ($\phi=1\%$) under a mid-spectrum flow rate. It clearly depicts that any element density more than 5×10^5 gives the variation of the simulation results in terms of Nu and ΔP are less than 1%. The selected mesh, detailed in Figure 1(b), consisted of 508,170 elements in total (355,880 in the fluid domain and 152,290 in the solid domain).

2.1.8 Model Validation

Reliability of the CFD model is established by comparing the results with the experimental data from the work of Vinoth and Sachuthanathan [20]. Simulation was conducted in a 1:5 scaled down geometry for flow rate range as described in the reference experiment both $\text{Al}_2\text{O}_3/\text{water}$ mono-nanofluid and $\text{Al}_2\text{O}_3+\text{CuO}/\text{water}$ hybrid nanofluid at various concentrations to validate current CFD model. This validation result has been shown in Figure 3. Pressure drop and average Nusselt number calculated based on current CFD model and experimental data are compared over a range of flow rates as described in the experiment. A close alignment of the simulated and experimental result to predict accurately the heat transfer and friction loss performance, gives a confidence to continue the remaining studies based on BN+SiC/Water hybrid nanofluid.

2.2 Parametric Study

The validated CFD model is used to study the performance of triangular oblique microchannel with BN+SiC/water hybrid nanofluid. The performance parameters of this heat sink are calculated in terms of friction factor (f), Nusselt number (Nu) and TPF. TPF is defined as $TPF = \frac{Nu_{nf}/Nu_{bf}}{(f_{nf}/f_{bf})^{1/3}}$. The parametric study is conducted to reveal the effects of nanoparticle concentration, mixing ratio, size, and shape on the performance parameters.

2.2.1 Concentration Study (BN+SiC / Water)

Sensitivity of total concentration of nanoparticles in the hybrid nanofluid and also the individual relative fractions of BN and SiC are studied to check the heat transfer, pressure drop and overall performance quantified in terms of Nu, f, and TPF respectively.

2.2.1.1 Investigating Total Concentration Effects

In this strategy, the total concentration of nanoparticles combining both BN and SiC in % of volume fraction (ϕ_{total}) varied from 0% (base fluid) to 1.5% at an increment of 0.25% [48] while keeping the mixing ratio of BN to SiC fixed at 1:1 for a specified range of flow rates (0.02 l/min to 0.1 l/min).

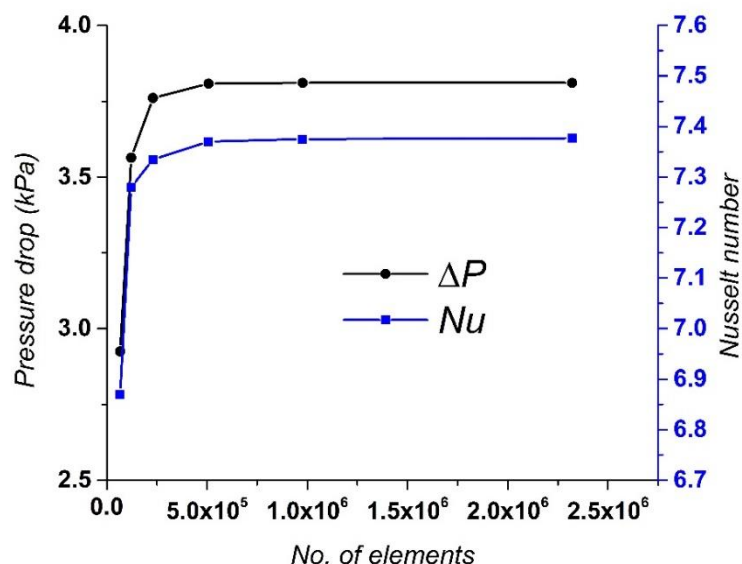


Figure 2. Grid independence study results showing Nu and ΔP vs. number of mesh elements

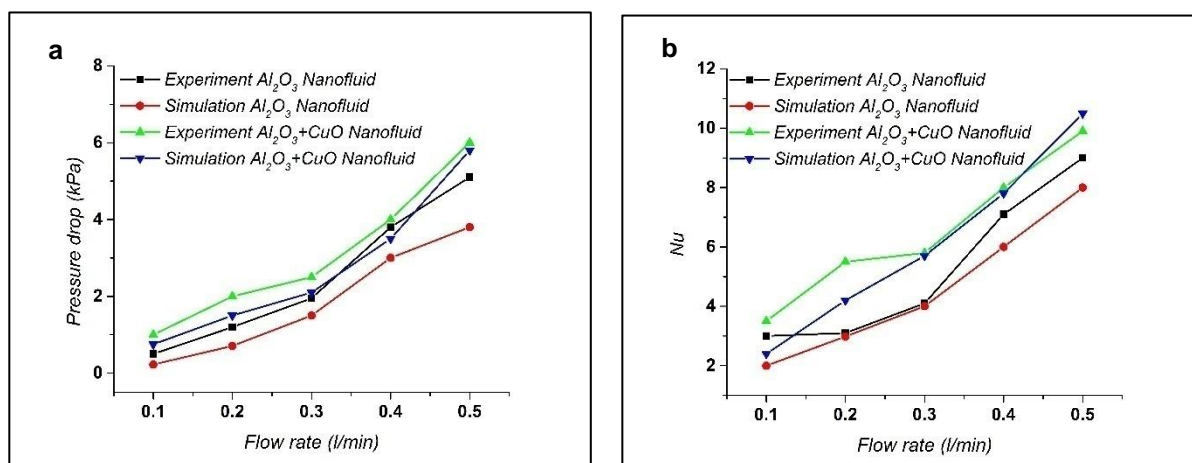


Figure 3. Model validation: Comparison of simulated vs. experimental [20] (a) Pressure Drop (b) Nusselt number for Al_2O_3 /water and Al_2O_3+CuO /water nanofluids

2.2.1.2 Examining Mixing Ratio Variations

In order to find the optimum mixing ratio of BN to SiC nanoparticles for a specified total volume fraction ($\phi_{total}=1\%$) a set of simulations were designed. Volumetric mixing ratio of BN to SiC were varied across the following proportions: 1 (100% BN and 0% SiC), 3:1 (75% BN and 25% SiC), 1:1 (50% BN and 50% SiC), 1:3 (25% BN and 75% SiC) and 0 (0% BN and 100% SiC). Simulations were conducted across the same flow rate range specified before.

2.2.2 Size & Structure Study (BN+SiC / Water)

The effect of nanoparticles' size and shape on the performance of the triangular oblique microchannel heat sink was studied for 1:1 mixing ratio of nanoparticles of BN to SiC and for optimum concentration of total volume fraction of nanoparticles from the prior study.

2.2.2.1 Size Effect (Diameter, d_{np})

In this simulations effect of nanoparticle size on thermo-hydraulic performance was examined assuming both BN and SiC nanoparticles are spherical in shape with average diameter (d_{np}) varied from 10nm to 90 nm at an uniform increment of 10nm. To incorporate the effect of particle diameter on thermal conductivity of nanofluid KKL model [45] was used where Brownian motion effect is inherent as shown in equation (9). These simulations were conducted at the flow rate of 0.1 l/min and for selected total volume fraction of nanoparticles of 0.5%, 1% and 1.5%. It is important to acknowledge that potential implications for nanofluid stability need careful consideration, as smaller particles generally offer better colloidal stability but can also exhibit different agglomeration behaviors [49].

2.2.2.2 Structure Effect (Shape)

This study was conducted to get an insight of the effect of realistic shapes of the nanoparticles on the thermo-hydraulic performance. Hamilton-Crosser model [44] (equation (8)) was utilized to evaluate the effective thermal conductivity based on shape parameters of the nanoparticles presented in Table 2. Krieger-Dougherty modified equation model [40] (equation 7(b)) was used to evaluate particle shape dependent effective viscosity of the nanofluid to check the influence of particle morphology on pressure drop and overall thermal performance. Spheres, nanorods, and platelets/flakes shapes of BN particles and spheres, nanorods, and whiskers for SiC were considered in our research over the specified range of flow rates and fixed mixing-ratio of 1:1 for total concentration volume fraction cases of 0.5%, 1% and 1.5%. Results were compared with the spherical assumed shapes and quantify the realistic shape influence on overall thermo-hydraulic performance.

3. Results and Discussion

The effects of nanoparticle concentration, BN to SiC mixing ratio, particle dimensions and morphology on the system's friction factor, average Nusselt number, and the Thermal Performance Factor are presented and analyzed in this section. Furthermore, the performance of the novel BN+SiC system is contrasted with a standard oxide-based hybrid nanofluid ($\text{Al}_2\text{O}_3+\text{CuO}/\text{water}$) under identical operational settings.

For a widely applicable analysis, the primary performance metrics of heat transfer and pressure drop were evaluated using their non-dimensional counterparts, the Nusselt number (Nu) and the Fanning friction factor (f). Since these non-dimensional parameters allow the results to be independent of the specific scale of the microchannel, they are frequently similar with those of earlier studies in the field.

The dimensional average heat transfer coefficient (h) and pressure drop (ΔP) can be calculated from these quantities. The heat transfer coefficient is derived from the Nusselt number using the relation $h = \frac{Nu k_{nf}}{D_h}$, where k_{nf} is the thermal conductivity of the nanofluid and D_h is the hydraulic diameter of the channel. Pressure drop is obtained from the friction factor via the equation $\Delta P = 2f \frac{l}{D_h} \rho_{nf} u_m^2$. Where, u_m =mean fluid velocity. Results are presented based on non-dimensional performance parameters Nu and f for relative performance potential rather than device-specific absolute values.

3.1 Effect of Total Nanoparticle Concentration (Fixed 1:1 Mixing Ratio)

Effect of variation of total volume fraction (ϕ_{total}) of BN and SiC combined for a fixed mixing ratio 1:1 of

BN to SiC on f, Nu and TPF across the investigated flow rates, were presented in Figure 4. Pure water (0% volume fraction of nanoparticles) is considered as reference base fluid, simulation results for the other concentrations (0.25% to 1.5% at an increment of 0.25%) are compared and analyzed based on data presented in Figure 4.

Friction factor consistently increases with the increase of total nanoparticle concentration is clearly observed from the Figure 4(a). On an average this increment across the range of flow rate and concentration (0.25% to 1.5%) is around 9% compared to base fluid water. This increasing trend is expected as the effective viscosity increases with particle concentration, consistent with the model correlation described in equation 7(a). Equation (5) clearly indicates that density increases with particle concentration, implies an increase in momentum responsible for higher pressure drop or non-dimensional friction factor to maintain the same flow rate.

An incremental trend is observed for the non-dimensional heat transfer performance parameter Nu with the increase of total concentration of nanoparticle loading. Average overall increment across the flow rate and concentration range is about 50%. This enhancement of thermal performance can be justified by the improvement of the effective thermal conductivity with the increase of particle concentration as per mathematical correlation shown in equation (8). Potential boundary layer modifications might offer secondary contributions, the enhanced thermal conductivity is typically the dominant factor in single-phase representations [50].

To understand the thermal benefit at the expense of pumping loss in practice, TPF comparison is plotted in Figure 4(c). It has been observed in general TPF increases with total concentration of nanoparticles in the specified range and a net gain in overall TPF on an average across the range of study is found to be around 20% in comparison to water. Thermal benefit dominates the frictional losses in this condition, implies a technically feasible cooling system solution provided the high concentration is well dispersed and stable in the base fluid.

In figure 5(a) comparative simulation data of friction factor and Nu of benchmark oxide hybrid $\text{Al}_2\text{O}_3+\text{CuO}/\text{water}$ system with non-oxide BN+SiC/water system is presented. Figure 5(b) compares the TPF of the same system benchmark oxide and non-oxide hybrid nanofluid over the specified range under the similar conditions. These data plots of these two figures reveals that thermal performance of BN+SiC system is enhanced by approximately 50% in comparison to 37% increment in Nu of $\text{Al}_2\text{O}_3+\text{CuO}$ system. Though friction factor in non-oxide system has been observed to increase by 9% in comparison to increment of 6% for oxide system.

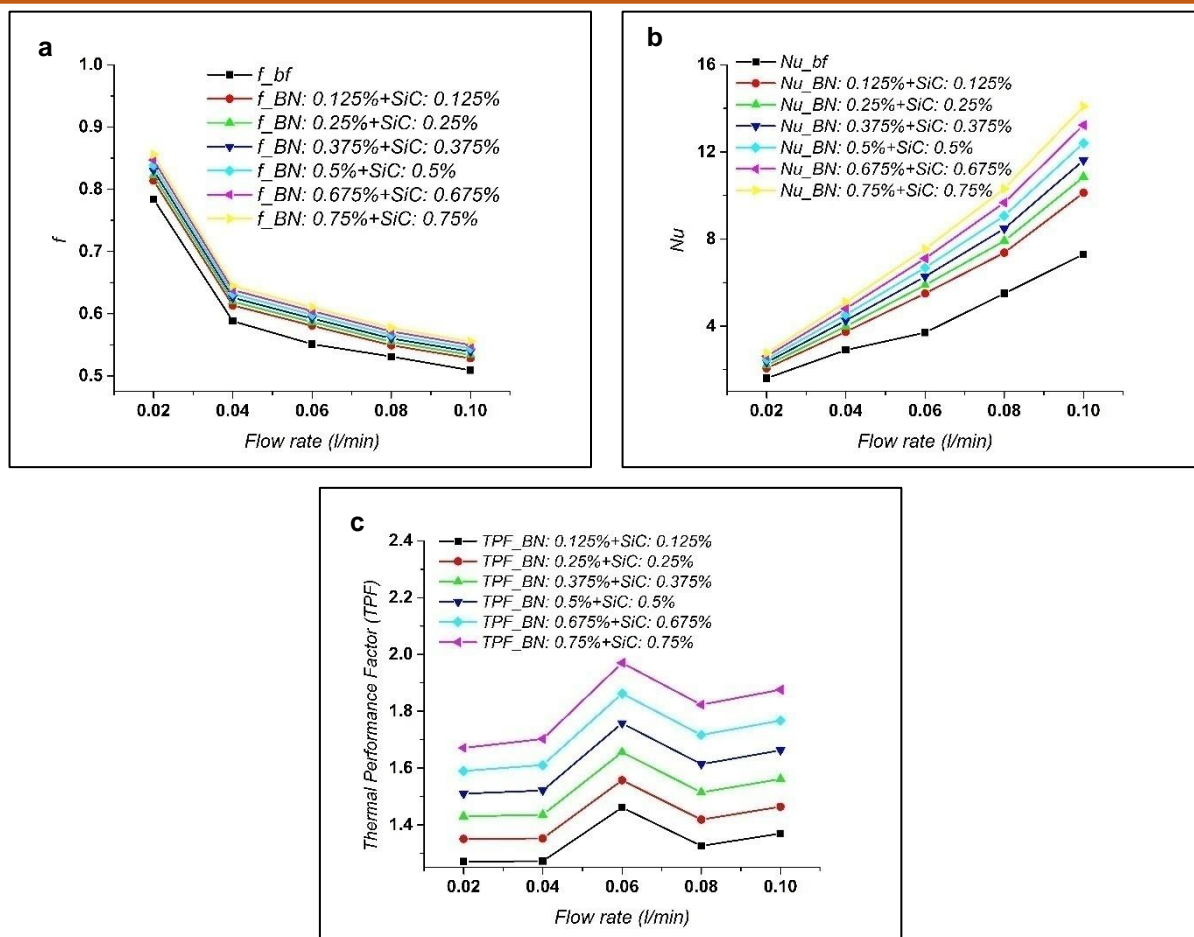


Figure 4. Effect of Total Concentration (ϕ_{total}) at 1:1 BN:SiC ratio on (a) Friction Factor, (b) Nusselt Number, (c) TPF

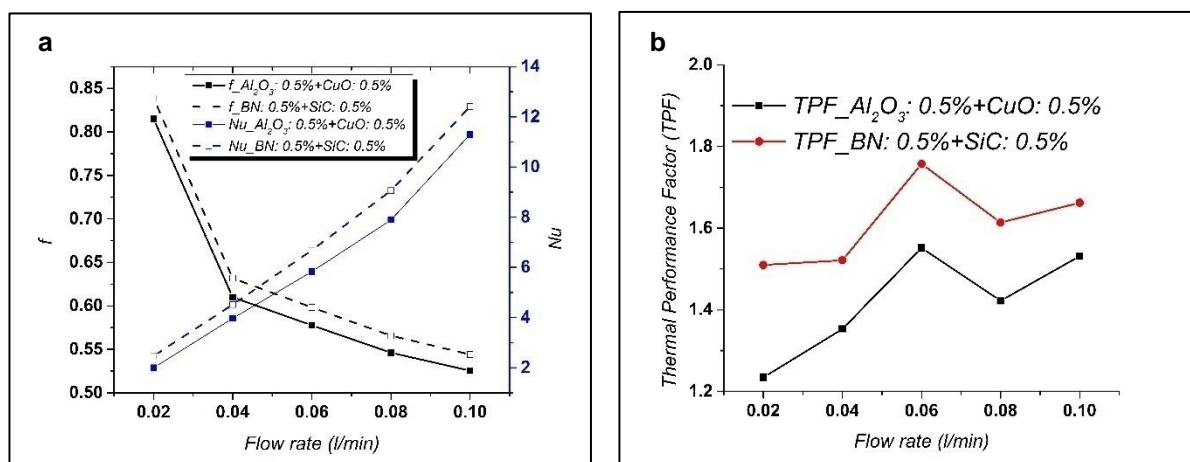


Figure 5. Thermo-hydraulic performance comparison of BN+SiC hybrid nanofluid with Al_2O_3+CuO (a) f & Nu (b) TPF

But TPF of non-oxide system is observed an enhancement of 20% in comparison to 10% for oxide system. The inherent thermal properties and possible beneficial synergistic interactions between BN and SiC likely account for this performance edge over the Al_2O_3+CuO pair, supporting the potential of BN+SiC fluids.

3.2 Effect of Mixing Ratio (Fixed Total Concentration)

Figure 6 displays the simulation results of the influence on performance parameters f , Nu and TPF due to variation of mixing ratio of BN to SiC (cases : 100:0, 75:25, 50:50, 25:75, 0:100) across the range of flow rates specified and for constant total concentration of 1% nanofluid.

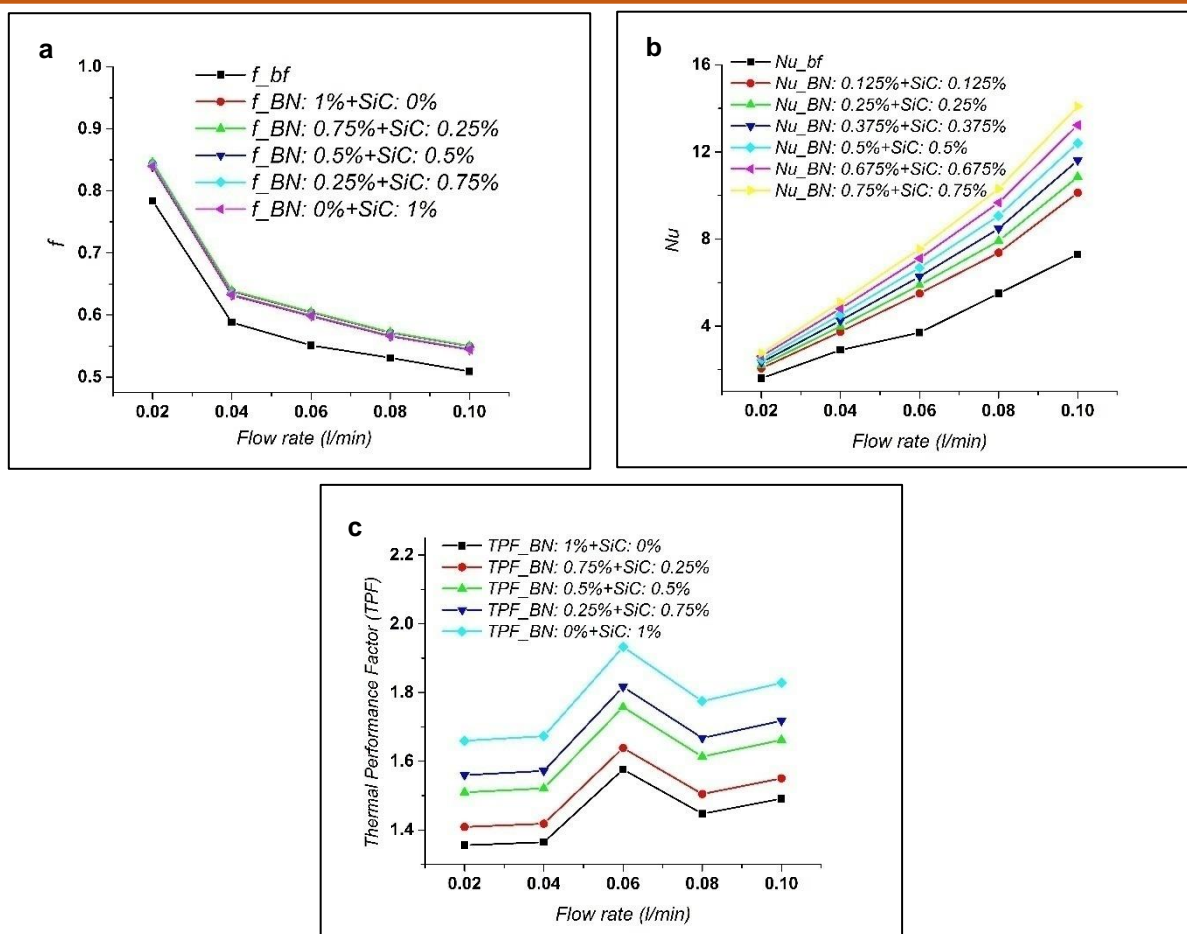


Figure 6. Effect of Mixing Ratio (at fixed $\phi_{total} = 1.0\%$) on (a) Friction Factor, (b) Nusselt Number, (c) Thermal Performance Factor

It has been observed from Figure 6(a) and 6(b) that across the complete range of study with the increase of relative proportion of SiC in the BN+SiC hybrid system friction factor and Nu both are increasing. Friction factor enhancement can be justified by the increase of fluid momentum with the relative increase of higher density SiC in compare to BN. High isotropic thermal conductivity of SiC, improves overall effective thermal conductivity of the nanofluid with the increase of SiC relative proportion, ultimately enhances thermal performance parameter Nu.

The TPF also followed an increasing trend as the SiC relative fraction increased (Figure (c)). This implies that the thermal enhancement benefit gained from incorporating more SiC effectively outweighs the rise in frictional losses. Within the scope of the tested ratios, these results suggest that maximizing SiC content yields the most favorable overall thermo-hydraulic performance.

3.3 Effect of Nanoparticle Size

Figure 7 shows the impact of nanoparticle size on the thermal performance of the hybrid nanofluid. It is observed that Nu increases monotonically with the decrease of the average nanoparticle diameter studied

in the range of 90nm to 10nm for a fixed flow rate of 0.1 l/min and 1:1 mixing ratio for three different total concentrations 0.5%, 1% and 1.5% respectively. This result is consistent with the literature [51] and can be explained by the fact that smaller particles have larger surface area for the same concentration of larger particles, increases heat transfer area. Again, Smaller particles enhance the heat transfer performance more because they are more actively involved in Brownian motion, responsible for high energy transport incorporated through the KKL model [45].

From a practical view, smaller particles also tend to offer better long-term suspension stability [52], although extremely small particles might face challenges with agglomeration if not properly stabilized.

3.4 Effect of Nanoparticle Shape

Acknowledging that real-world nanoparticles often possess non-spherical morphologies; our final parametric evaluation examined the impact of particle shape. Various combinations were considered such as BN as spheres, nanorods, or flakes, and SiC as spheres, nanorods, or whiskers at a 1.0% total concentration and a 1:1 mixing ratio.

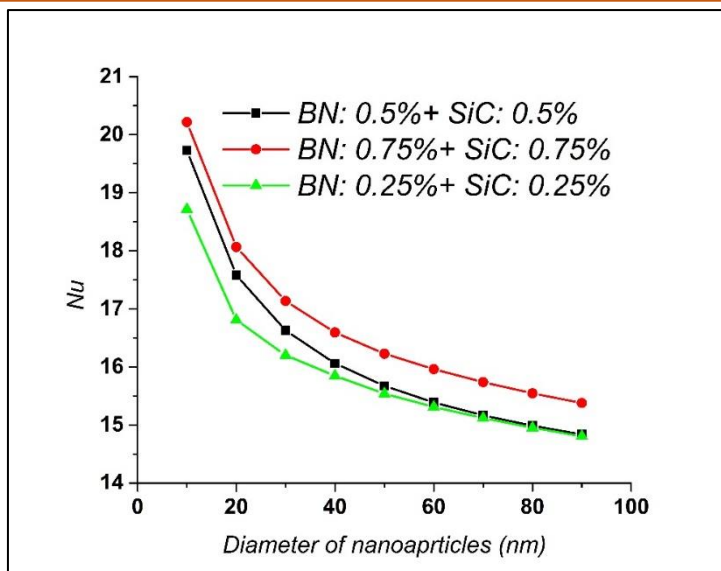


Figure 7. Effect of Nanoparticle Diameter (d_{np} , assuming spherical BN and SiC) on Nusselt Number for different ϕ_{total} (at 1:1 mixing ratio, 0.1 l/min fixed flow rate)

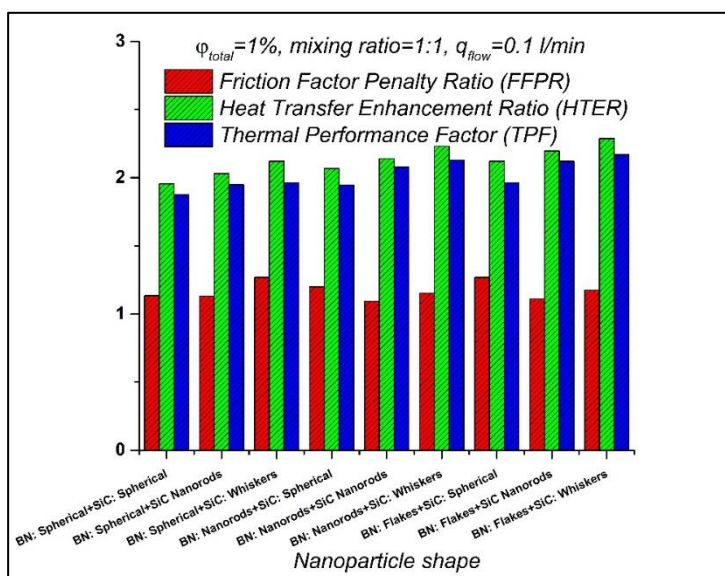


Figure 8. Bar chart comparing the effect of different BN and SiC nanoparticle shape combinations

Shape-dependent property models, notably the Hamilton-Crosser model for thermal conductivity (equation (8)) using relevant shape factors (n), were applied. Figure provides an overview comparing the Friction Factor Penalty Ratio ($FFPR = \frac{f_{nf}}{f_{bf}}$), Heat Transfer Enhancement Ratio ($HTER = \frac{Nu_{nf}}{Nu_{bf}}$), and TPF across different shape pairings.

Nanoparticle shape profoundly influences both flow resistance and heat transfer. As shown in Figure , while all combinations increased FFPR relative to water, those pairing a high-aspect-ratio particle (whisker, flake, nanorod) with a sphere generally incurred higher penalties due to increased hydrodynamic drag. Conversely, significant HTER improvements were observed, particularly when both particle types were non-spherical (e.g., BN: Nanorods+ SiC: Whiskers, BN: Flakes+ SiC: Nanorods/Whiskers). Thermal

performance can be enhanced by large surface area, increased probability of micro-mixing and by formation of highly conducting network. These features can be related to the shape effect on thermo-physical properties [44]. The most favorable combination of BN and SiC structures based on the TPF is found to be flakes or nanorods of BN and whiskers or nanorods of SiC. These can be concluded from this observation that high aspect ratio shape particles are having high overall performance considering both thermal benefit and hydraulic loss. The optimal choice depends on the type of application. However, the enhanced TPF of non-spherical combinations are having potential long-term stability challenges, as these shapes are often more susceptible to aggregation [49].

3.5 Practical Implications and Stability Considerations

In this research it has been observed that optimized combination of BN and SiC with high aspect ratio combinations are beneficial over the existing nanofluid systems. But non spherical particles can agglomerate and settle easily in the microchannel flow path if not properly stabilized and can degrade the overall thermo-hydraulic performance. Ensuring durable and uniform dispersion is therefore of primary importance and will likely require advanced stabilization strategies, including nanoparticle surface functionalization or precise control of suspension pH. Viscosity increment over time can also increase the pumping loss, need to be considered in practice. Hard SiC can also erode the channel surface over time is also a concern in application. The mentioned challenges are not covered in this numerical study.

This work provides a strong theoretical basis and highlights the potential of nanoparticle shape customization, future research must focus on long-term performance assessment and experimental validation. Developing robust stabilization methods and systematically assessing stability under realistic operating conditions will be essential steps toward the practical deployment of BN+SiC hybrid nanofluids in next generation cooling systems.

4. Conclusion

This research work revealed the novel non-oxide hybrid (BN+SiC/water) nanofluid potential as a heat transfer fluid in a systematic numerical parametric study in a complex oblique triangular section microchannel.

Effect of total concentration of BN and SiC in water (over a range from 0.5% to 1.5%) on f , Nu and TPF are studied and found enhancement in Nu of 50%, friction factor by 9% and TPF by 20% in comparison to pure water. Results are also compared with the benchmark oxide hybrid nanofluid ($Al_2O_3+CuO/water$) at the similar conditions and it is found that BN+SiC system are better heat transfer fluid considering overall thermal efficiency. For fixed total concentration of nanoparticles, effect of mixing ratio of BN to SiC on performance parameters have been studied. It can be concluded from the results that enhancement of Nu and TPF is observed for higher relative proportion of SiC for its higher intrinsic thermal conductivity. Size effect on the performance parameters are also studied and results revealed that reducing the diameter of nanoparticles from 90nm to 10nm enhances the Nu. Effect of morphology of the nanoparticles are also studied concluded that the high aspect ratio particle shapes are more beneficial for overall thermal performance. Combining BN Nanorods with SiC Whiskers yielded the optimal TPF, balancing thermal gains and frictional penalties.

This detail parametric study of novel BN+SiC/water system contribute in field of ever-increasing challenge of advanced cooling system design by customizing the structure, size, relative and total concentration of nanoparticles to use as per requirement. Definitely before commercialization further experimental validation for long term stability, performance and rheological studies are required.

This highly potential hybrid nanofluid combination with complex microchannel geometry is a novel cooling solution of the current continuous evolving high heat flux devices like data center hardware, high energy battery pack and fast charger etc. This research can be extended by further studies using two-phase model for high concentration nanofluid and also capturing anisotropic characteristics of h-BN in the model, would give a more insight of the system. An experimental synthesis and characterization of this newly suggested BN+SiC system is required along with proper stability analysis. These efforts are essential for the practical implementation of BN+SiC nanofluids in thermal management systems.

References

- [1] K.P. Bloschock, A. Bar-Cohen, Advanced thermal management technologies for defense electronics. In Defense Transformation and Net-Centric Systems, SPIE, 8405, (2012) 157-168. <https://doi.org/10.1117/12.924349>
- [2] K.W. Jung, C. Zhang, T. Liu, M. Asheghi, K. E. Goodson, Thermal Management Research – from Power Electronics to Portables. in 2018 IEEE Symposium on VLSI Technology, IEEE, USA. <https://doi.org/10.1109/VLSIT.2018.8510678>
- [3] A. R. Dhumal, A.P. Kulkarni, N.H. Ambhore, A comprehensive review on thermal management of electronic devices. Journal of Engineering and Applied Science, 70(1), (2023) 140. <https://doi.org/10.1186/s44147-023-00309-2>
- [4] S. Jones-Jackson, R. Rodriguez, Y. Yang, L. Lopera, A. Emadi, Overview of Current Thermal Management of Automotive Power Electronics for Traction Purposes and Future Directions. IEEE Transactions on Transportation Electrification, 8(2), (2022) 2412–2428. <https://doi.org/10.1109/TTE.2022.3147976>
- [5] N. Czaplicka, A. Grzegórska, J. Wajs, J. Sobczak, A. Rogala, Promising Nanoparticle-Based Heat Transfer Fluids—Environmental and Techno-Economic Analysis Compared to Conventional Fluids. International Journal of Molecular Sciences, 22(17), (2021) 9201. <https://doi.org/10.3390/ijms22179201>
- [6] P. Bhandari, K.S. Rawat, Y.K. Prajapati, D. Padalia, L. Ranakoti, T. Singh, Design modifications in micro pin fin configuration of

- microchannel heat sink for single phase liquid flow: A review. *Journal of Energy Storage*, 66, (2023) 107548. <https://doi.org/10.1016/j.est.2023.107548>
- [7] S. Kandlikar, (2006). *Heat Transfer and Fluid Flow in Minichannels and Microchannels*. Elsevier.
- [8] A. Jebelli, N. Lotfi, M.S. Zare, M.C.E. Yagoub, Advanced Thermal Management for High-Power ICs: Optimizing Heatsink and Airflow Design. *Applied Sciences*, 14(20), (2024) 9406. <https://doi.org/10.3390/app14209406>
- [9] S.K. Das, S.U. Choi, W. Yu, T. Pradeep, (2007) *Nanofluids: Science and Technology*. John Wiley & Sons.
- [10] S.U. Choi, J.A. Eastman, (1995) Enhancing thermal conductivity of fluids with nanoparticles. Argonne National Lab. (ANL), Argonne, IL United States.
- [11] N. Abdullah, W.M.D.Z.W. Yunus, I.S. Mohamad, Thermal Conductivity Comparisons of Original And Oxidized Multiwalled Carbon Nanotubes-Waterbased Fluids. *Jurnal Teknologi*, 76(9), (2015). <https://doi.org/10.11113/jt.v76.5645>
- [12] F. Mebarek-Oudina, I. Chabani, Review on Nano-Fluids Applications and Heat Transfer Enhancement Techniques in Different Enclosures. *Journal of Nanofluids*, 11(2), (2022) 155–168. <https://doi.org/10.1166/jon.2022.1834>
- [13] S. Zeinali Heris, M. Nasr Esfahany, S. Gh. Etemad, Experimental investigation of convective heat transfer of Al₂O₃/water nanofluid in circular tube. *International Journal of Heat and Fluid Flow*, 28(2), (2007) 203–210. <https://doi.org/10.1016/j.ijheatfluidflow.2006.05.001>
- [14] J. Wang, X. Yang, J.J. Klemeš, K. Tian, T. Ma, B. Sunden, A review on nanofluid stability: preparation and application. *Renewable and Sustainable Energy Reviews*, 188, (2023) 113854. <https://doi.org/10.1016/j.rser.2023.113854>
- [15] S.N.M. Zainon, W.H. Azmi, Recent Progress on Stability and Thermo-Physical Properties of Mono and Hybrid towards Green Nanofluids. *Micromachines*, 12(2), (2021) 176. <https://doi.org/10.3390/mi12020176>
- [16] A. Bin Mahfouz, A. Ali, M. Mubashir, A.S. Hanbazazah, M. Alsaady, P.L. Show, Optimization of viscosity of titania nanotubes ethylene glycol/water-based nanofluids using response surface methodology. *Fuel*, 347, (2023) 128334. <https://doi.org/10.1016/j.fuel.2023.128334>
- [17] S.A. Nada, R.M. El-Zoheiry, M. Elsharnoby, O.S. Osman, Enhancing the thermal performance of different flow configuration minichannel heat sink using Al₂O₃ and CuO-water nanofluids for electronic cooling: An experimental assessment. *International Journal of Thermal Sciences*, 181, (2022) 107767. <https://doi.org/10.1016/j.ijthermalsci.2022.107767>
- [18] A.K. Jouybari, S. Dinarvand, P. Tehrani, M.E. Yazdi, G. Salehi, Turbulent Flow and Heat Transfer of Al₂O₃–CuO Hybrid Nanofluids in Helically Micro-Finned Tubes Using Mass-Based and Discrete-Phase Models. *Journal of Nanofluids*, 13(5), (2024) 1134–1144. <https://doi.org/10.1166/jon.2024.2199>
- [19] S. Zeinali Heris, N. Zolfagharian, S.B. Mousavi, S. Hosseini Nami, Enhancing the synergistic properties of plate heat exchangers using nanohybrid MWCNTs–SiO₂ EG-based nanofluids. *Journal of Thermal Analysis and Calorimetry*, 150(8), (2025) 6225–6244. <https://doi.org/10.1007/s10973-025-14165-0>
- [20] R. Vinoth, B. Sachuthananthan, Flow and heat transfer behavior of hybrid nanofluid through microchannel with two different channels. *International Communications in Heat and Mass Transfer*, 123, (2021) 105194. <https://doi.org/10.1016/j.icheatmasstransfer.2021.105194>
- [21] S. Kumar, A.K. Tiwari, Performance evaluation of evacuated tube solar collector using boron nitride nanofluid. *Sustainable Energy Technologies and Assessments*, 53, (2022) 102466. <https://doi.org/10.1016/j.seta.2022.102466>
- [22] M. Farbod, Z. Rafati, Heat transfer, thermophysical and rheological behavior of highly stable few-layers of h-BN nanosheets/EG-based nanofluid. *Materials Today Communications*, 33, (2022) 104921. <https://doi.org/10.1016/j.mtcomm.2022.104921>
- [23] Z. Duan, Z. Wang, Y. Jia, S. Wang, P. Bian, J. Tan, J. Song, X. Liu, Dispersion Stability and Tribological Properties of Cold Plasma-Modified h-BN Nanofluid. *Nanomaterials*, 15(11), (2025) 874. <https://doi.org/10.3390/nano15110874>
- [24] A.K. Tiwari, Z. Said, N.S. Pandya, H. Shah, Effect of plate spacing and inclination angle over the thermal performance of plate heat exchanger working with novel stabilized polar solvent-based silicon carbide nanofluid. *Journal of Energy Storage*, 60, (2023) 106615. <https://doi.org/10.1016/j.est.2023.106615>
- [25] C. Guo, Z. Wu, X. Wang, J. Zhang, Comparison in performance by emulsion and SiC nanofluids HS-WEDM multi-cutting process. *The International Journal of Advanced Manufacturing Technology*, 116(9), (2021) 3315–3324. <https://doi.org/10.1007/s00170-021-07600-7>
- [26] A.H. Shaik, S. Chakraborty, S. Saboor, K.R. Kumar, A. Majumdar, M. Rizwan, M. Arıcı, M.R. Chandan. Cu-Graphene water-based hybrid nanofluids: synthesis, stability, thermophysical

- characterization, and figure of merit analysis. *Journal of Thermal Analysis and Calorimetry*, 149(7), (2024) 2953–2968. <https://doi.org/10.1007/s10973-023-12875-x>
- [27] R. Peng, X. Chen, M. Zhou, L. Zhao, J. Gao, Process optimization via synergistic hBN/SiC nanofluid and internal cooling for low-damage grinding of Inconel 718. *Ceramics International*, 51(24), (2025) 43436–43450. <https://doi.org/10.1016/j.ceramint.2025.07.083>
- [28] L. Du, W. Hu, An overview of heat transfer enhancement methods in microchannel heat sinks. *Chemical Engineering Science*, 280, (2023) 119081. <https://doi.org/10.1016/j.ces.2023.119081>
- [29] S. S. Mousavi Ajarostaghi, M. Zaboli, H. Javadi, B. Badenes, J.F. Urchueguia, A Review of Recent Passive Heat Transfer Enhancement Methods. *Energies*, 15(3), (2022) 986. <https://doi.org/10.3390/en15030986>
- [30] W. Mohd. A.A. Japar, N.A.C. Sidik, R. Saidur, Y. Asako, S. Nurul Akmal Yusof, A review of passive methods in microchannel heat sink application through advanced geometric structure and nanofluids: Current advancements and challenges. *Nanotechnology Reviews*, 9(1), (2022) 1192–1216. <https://doi.org/10.1515/ntrev-2020-0094>
- [31] Y. Alihosseini, M. Zabetian Targhi, M. Mahdi Heyhat, Thermo-hydraulic performance of wavy microchannel heat sink with oblique grooved finned. *Applied Thermal Engineering*, 189, (2021) 116719. <https://doi.org/10.1016/j.applthermaleng.2021.116719>
- [32] Y.J. Lee, P.S. Lee, S.K. Chou, (2009) Enhanced Microchannel Heat Sinks Using Oblique Fins. ASME 2009 InterPACK Conference collocated with the ASME 2009 Summer Heat Transfer Conference and the ASME 2009 3rd International Conference on Energy Sustainability, International Electronic Packaging Technical Conference and Exhibition, California, USA. <https://doi.org/10.1115/InterPACK2009-89059>
- [33] V. Kumar, J. Sarkar, Numerical Analysis on Hydrothermal Behavior of Various Ribbed Minichannel Heat Sinks with Different Hybrid Nanofluids. *Arabian Journal for Science and Engineering*, 47(5), 6209–6221. <https://doi.org/10.1007/s13369-021-06119-z>
- [34] S. Borah, D. Bhanja, Enhancing thermo-hydraulic performance in flow boiling with hybrid nanofluids in double-layered wavy microchannel heat sink. *Applied Thermal Engineering*, 273, (2025)126488. <https://doi.org/10.1016/j.applthermaleng.2025.126488>
- [35] S.V. Patankar, (2018) Numerical Heat Transfer and Fluid Flow, 1st ed. CRC Press. <https://doi.org/10.1201/9781482234213>
- [36] G. Hetsroni, A. Mosyak, Z. Segal, G. Ziskind, A uniform temperature heat sink for cooling of electronic devices. *International Journal of Heat and Mass Transfer*, 45(16), (2002) 3275–3286. [https://doi.org/10.1016/S0017-9310\(02\)00048-0](https://doi.org/10.1016/S0017-9310(02)00048-0)
- [37] M.M. Rashidi, M.A. Nazari, I. Mahariq, M.E.H. Assad, M.E. Ali, R. Almuzaqer, A. Nuhait, N. Murshid, Thermophysical properties of hybrid nanofluids and the proposed models: An updated comprehensive study. *Nanomaterials*, 11(11), (2021) 3084. <https://doi.org/10.3390/nano11113084>
- [38] Y. Xuan, W. Roetzel, Conceptions for heat transfer correlation of nanofluids. *International Journal of Heat and Mass Transfer*, 43(19), (2000) 3701–3707. [https://doi.org/10.1016/S0017-9310\(99\)00369-5](https://doi.org/10.1016/S0017-9310(99)00369-5)
- [39] H.C. Brinkman, The Viscosity of Concentrated Suspensions and Solutions. *The Journal of Chemical Physics*, 20(4), (1952) 571. <https://doi.org/10.1063/1.1700493>
- [40] I.M. Krieger, T.J. Dougherty, A Mechanism for Non-Newtonian Flow in Suspensions of Rigid Spheres. *Transactions of the Society of Rheology*, 3(1), (1959) 137–152. <https://doi.org/10.1122/1.548848>
- [41] Y. Wang, W. Zhang, M. Feng, M. Qu, Z. Cai, G. Yang, Y. Pan, C. Liu, C. Shen, X.Liu. The influence of boron nitride shape and size on thermal conductivity, rheological and passive cooling properties of polyethylene composites. *Composites Part A: Applied Science and Manufacturing*, 161, (2022) 107117. <https://doi.org/10.1016/j.compositesa.2022.107117>
- [42] R. Mondragon, J. Enrique Julia, A. Barba, J.C. Jarque, Determination of the packing fraction of silica nanoparticles from the rheological and viscoelastic measurements of nanofluids. *Chemical Engineering Science*, 80, (2012) 119–127. <https://doi.org/10.1016/j.ces.2012.06.009>
- [43] W.K. Zhen, Z.Z. Lin, C.L. Huang, Modified Maxwell model for predicting thermal conductivity of nanocomposites considering aggregation. *Chinese Physics B*, 26(11), (2017) 114401. <https://doi.org/10.1088/1674-1056/26/11/114401>
- [44] R.L. Hamilton, O.K. Crosser Thermal conductivity of heterogeneous two-component systems. *Industrial & Engineering chemistry fundamentals*, 1(3), (1962) 187–191. <https://doi.org/10.1021/i160003a005>
- [45] J. Koo, C. Kleinstreuer, A new thermal conductivity model for nanofluids. *Journal of Nanoparticle research*, 6(6), (2004) 577–588. <https://doi.org/10.1007/s11051-004-3170-5>
- [46] E.W. Lemmon, (2010) Thermophysical properties of fluid systems. NIST chemistry

WebBook.

- [47] D.R. Lide, G. Baysinger, S. Chemistry, L.I. Berger, R. N. Goldberg, and H.V. Kehiaian, (1995) CRC Handbook of Chemistry and Physics.
- [48] M. Malý, A.S. Moita, J. Jedelsky, A.P.C. Ribeiro, A.L.N. Moreira, Effect of nanoparticles concentration on the characteristics of nanofluid sprays for cooling applications. Journal of Thermal Analysis and Calorimetry, 135(6), (2019) 3375-3386. <https://doi.org/10.1007/s10973-018-7444-z>
- [49] W. Yu, H. Xie, A review on nanofluids: preparation, stability mechanisms, and applications. Journal of nanomaterials, 2012(1), (2012) 435873. <https://doi.org/10.1155/2012/435873>
- [50] X.Q. Wang, A.S. Mujumdar, Heat transfer characteristics of nanofluids: a review. International journal of thermal sciences, 46(1), (2007) 1-19. <https://doi.org/10.1016/j.ijthermalsci.2006.06.010>
- [51] I.U. Ibrahim, M. Sharifpur, J.P. Meyer, S.S. Murshed, Experimental investigations of effects of nanoparticle size on forced convective heat transfer characteristics of Al₂O₃-MWCNT hybrid nanofluids in transitional flow regime. International Journal of Heat and Mass Transfer, 228, (2024)125597. <https://doi.org/10.1016/j.ijheatmasstransfer.2024.125597>
- [52] S. Mukherjee, S. Chakrabarty, P.C. Mishra, P. Chaudhuri, Stability and sedimentation characteristics of water based Al₂O₃ and TiO₂ nanofluids. Proceedings of the Institution of Mechanical Engineers, Part N: Journal of Nanomaterials, Nanoengineering and Nanosystems, 238, (2024) 17–30. <https://doi.org/10.1177/23977914221127735>

Data Availability

The data supporting the findings of this study can be obtained from the corresponding author upon reasonable request.

Has this article screened for similarity?

Yes

About the License

© The Author(s) 2026. The text of this article is open access and licensed under a Creative Commons Attribution 4.0 International License.

Authors Contribution Statement

Anirban Bose: Conceptualization, Methodology, Investigation, Formal analysis, Writing - Original Draft, Writing - Review & Editing. Arunabha Chanda: Investigation, Formal analysis, Writing - Review & Editing. Both the authors have read and agreed to the published version of the manuscript.

Funding

The authors declare that no funds, grants or any other support were received during the preparation of this manuscript.

Competing Interests

The authors declare that there are no conflicts of interest regarding the publication of this manuscript.